Surface Science 580 (2005), 80-94

In-situ X-ray photoelectron spectroscopy study of the oxidation of $CuGaSe_2$

R. Würz [a,*], M. Rusu [a], Th. Schedel-Niedrig [a,*], M. Ch. Lux-Steiner [a]
H. Bluhm [b], M. Hävecker [b], E. Kleimenov [b], A. Knop-Gericke [b], R. Schlögl [b]

[a] Hahn-Meitner Institut Berlin, Abteilung SE2, Glienicker Str. 100, 14109 Berlin, Germany
[b]Department of Inorganic Chemistry, Fritz-Haber-Institute of the MPG, Faradayweg 4-6, 14195 Berlin, Germany

[*] Corresponding authors: e-mail wuerz-r@hmi.de, schedel-niedrig@hmi.de
phone +49 30 8062 3243, fax +49 30 8062 3199

Received: 19 july 2004, accepted for publication 27 january 2005

Abstract

The thermal and native oxidation of $CuGaSe_2$ thin films was studied by in-situ X-ray photoelectron spectroscopy (XPS). The special design of the XPS chamber allowed to measure XP-spectra under oxidizing gas atmospheres at pressures of up to 5mbar (in-situ) or in ultra high vacuum (UHV). During thermal oxidation, the formation of predominantly Ga_2O_3 and some amount of SeO_2 were observed, but no copper oxides could be detected in the near surface region of the thin films. The same oxides were found after native oxidation in air under ambient conditions. Only after long term native oxidation for longer than four months $Cu(OH)_2$ was detected. An additional sodium oxide compound formed at the thin film surface, Na_xO and Na_2CO_3 after thermal and native oxidation, respectively. The amount of these sodium oxide compounds depends on the Na content on the as prepared surface. The formation of SeO_2 under humid conditions at 100°C was found to depend on the surface composition of the thin film.

Keywords: $CuGaSe_2$; sodium; chalcopyrite; oxidation; photoelectron spectroscopy, polycrystalline surfaces.

1. Introduction

$CuGaSe_2$ belongs to the class of *I-III-VI*$_2$ semiconducting chalcopyrites. With its high bandgap of $E_g = 1.68$eV at room temperature and optical absorption coefficient larger than 10^4cm^{-1} for photon energies $h\nu > 1.7$eV, $CuGaSe_2$ is a promising absorber for thin-film solar cell devices. Up to now energy conversion efficiencies of 9.7% and 9.5% have already been achieved for single-crystal [1] and thin-film cells [2], respectively. A pronounced degradation of ZnO/CdS/$CuGaSe_2$ solar cells was found, when the $CuGaSe_2$ absorber films were exposed to air before deposition of CdS [3]. Exposure to humid air before CdS deposition even accelerates the degradation process in case of Cu(In,Ga)Se_2 solar cells [4]. It is concluded, that oxidation in air deteriorates the solar cell performance. Despite these observations, no oxidation studies of $CuGaSe_2$ could be found in literature. Only $CuInSe_2$ and Cu(In,Ga)Se_2 are the most investigated materials from the copper containing class of chalcopyrites. Surface sensitive XPS is applied in order to study, which oxide phases form during the oxidation process. During thermal oxidation of $CuInSe_2$ crystals and thin films Kazmerski et al. [5] found formation of mainly In_2O_3 and some SeO_2, but no copper oxide. Further a Cu_xSe transition layer was found between the oxide layer and $CuInSe_2$ [5]. The native oxidation of $CuInSe_2$ takes place in the same way [6, 7]. Only at higher humidity some amount of Cu_xO was detected at the surface of the thin native oxides [6]. When oxidizing Cu(In,Ga)Se_2 films [4, 8], predominantly Ga_2O_3, In_2O_3 and some amount of SeO_2 formed, but no Cu_xO was observed.

In this paper we will study the formation of thermal and native oxides on $CuGaSe_2$ thin film surfaces with XPS. In contrast to the thermal oxides we observe formation of a $Cu(OH)_2$ phase at the surface of thin films after native oxidation for longer than four months. Details of the oxidation process as a function of the composition of the films will be presented. Spectra measured in gas atmosphere will be

compared with those measured afterwards in vacuum. The results will be discussed in the framework of a simplified model for the oxidation process.

2. Experimental

Thin polycrystalline films of $CuGaSe_2$ were grown by chemical close-spaced vapor transport (CCSVT) [9]. The soda lime glass substrates were covered with a 750 nm thick Mo layer and a 250 nm thick Cu layer by electron beam evaporation. Polycrystalline Ga_2Se_3 – synthesized from the elements – was subjected to a continuous flow of H_2/HCl and volatilized due to chemical reactions at a source temperature of 550°C. The resulting gases GaCl, $GaCl_2$, $GaCl_3$ and H_2Se then reacted on the substrate with the Cu precursor layer at a temperature of 450°C to $CuGaSe_2$ (for details see [9]). In a second annealing step the HCl flux was reduced to allow fine tuning of the thickness and the [Ga]/[Cu]-ratio of the resulting $Cu_xGa_ySe_2$ films [9]. Alternatively $CuGaSe_2$ thin films were grown on Mo coated soda lime glass substrates by halogen supported chemical vapor deposition (CVD) in an open tube system. Polycrystalline binary source materials Cu_2Se and Ga_2Se_3 – synthesized from the elements – were subjected to continuous flows of H_2/I_2 and H_2/HCl, respectively, and volatilized due to chemical reactions at a source temperature of 600°C and at a reactor pressure of 100 mbar. The resulting gases CuI, $GaCl_x$ (x = 1, 2, 3) and H_2Se were injected into the substrate zone where they were mixed and cooled down to 500°C leading to chemical reactions into the solid phase [10]. By adjusting the flow rates [11] or by a two-stage process [12] the [Ga]/[Cu]-ratio of the resulting $Cu_xGa_ySe_2$ films can be controlled.

Selected samples were transported in inert Ar gas atmosphere from the reactor to the XPS setup to avoid oxidation and to get reference spectra of as prepared samples. Only during mounting onto the sample holder and transfer into the chamber, these samples were exposed to air for about 20 min.

XPS measurements were carried out with synchrotron radiation at beamline U49/2-PGM1 at BESSY II in Berlin [13] using a high-pressure X-ray photoelectron spectrometer that allows measurements at pressures of up to 5mbar [14]. In addition a conventional X-ray photoelectron spectroscopy setup with a MgK_α X-ray source was used. In the synchrotron-based measurements the incident photon energy for excitation was chosen such that the kinetic energy of the emitted photoelectrons was about 300eV, i.e. the information depth was comparable in all spectra. The photon energy was calibrated by measuring the Fermi energy of the sample holder. The C1s signal from adventitious carbon with a binding energy $E_B = 285$eV was also used for energy referencing. The combined energy resolution of the beamline and the electron analyzer was ≈ 0.2eV at a pass energy of 10eV. All spectra were normalized by the incident photon flux, which was measured using a photodiode with known quantum efficiency. A linear background was subtracted from the spectra.

The thermal oxides were grown in-situ in dry oxygen at a pressure of 0.5mbar or in humid oxygen adding water vapor with a partial pressure of 0.2mbar inside the high-pressure cell of the XPS setup. During the XPS measurements the incident photon beam is admitted to this cell through a silicon nitride window with a thickness of 100nm that separates the high pressure region in the cell from the UHV environment in the beamline. The sample surface is placed close to a small aperture (1mm diameter) that is the entrance to a three-stage differentially-pumped electrostatic transfer lens. Electrons that escape through the first aperture are subsequently focussed onto two additional apertures downstreams before reaching a conventional hemispherical analyzer. This three-stage differentially-pumped electrostatic lens system allows to measure samples at pressures of several mbar, while the hemispherical analyzer is kept at pressures of 10^{-8}mbar [14]. Using this high-pressure spectrometer XPS measurements were performed during the oxidation of the thin films in the gas atmosphere at different oxidation temperatures T_{ox}, as well as afterwards in vacuum. Before starting the XPS measurements in gas atmosphere, the samples were exposed to the gas for about 30min to ensure that an oxide had formed. The native oxides were grown by storing the films in air under ambient conditions at room temperature for several months. The bulk chemical composition and the thickness of the films was determined by X-ray fluorescence spectrometry (XRF) using a Philips MagicsPRO spectrometer. Details of the samples studied here and the various treatments are listed in table 1.

3. Results

Before oxidation of as prepared thin films (sample #1 and #2) their contamination was checked, as they were exposed to air during mounting on the sample holder. Oxygen and carbon adsorbed on the film surface were found to be the main contaminants. The peak positions of the $Cu2p_{3/2}$, Ga3d and the $Se3d_{5/2}$ level of 932.2eV, 19.4eV and 53.7eV, respectively, correspond to the literature data of as grown samples [15]. Therefore we can assume the surface of the as prepared samples essentially to be free of any oxide phases containing Cu, Ga or Se. This is also supported by the Auger spectra (not shown). In table 2 the relative composition data of the near surface region, obtained by an XPS line analysis, as well as that of the bulk, determined by XRF, are listed. The XPS line area analysis was done by using the core level photoionization cross sections from Yeh et al. [16] and assuming, that the product of the analyzer transmission function and the inelastic mean free path is constant for our spectrometer at the utilized kinetic energies and pass energies. All XPS data in table 2 are given relative to the Cu content (set to one) with a relative error of ~10%. The surface composition (XPS) of sample #1 and #2 strongly deviates from the bulk composition

Table 1: $CuGaSe_2$ samples used for XPS measurements and their oxidation process together with the oxidation temperature T_{ox}, oxidation time, gas atmosphere and gas pressure during oxidation. Here " humid O_2" means 0.5mbar O_2 and 0.2mbar H_2O. The bulk [Ga]/[Cu]-ratio was determined by XRF. Samples with the same number stem from the same substrate.

sample	[Ga]/[Cu]	growth method	oxide	T_{ox} / °C	oxidation time	gas atmosphere	pressure/mbar
#1	1.032 ± 0.025	CCSVT	thermal	100	90 min	humid O_2	0.7
				200	85 min	O_2	0.7
				300	70 min	O_2	0.7
#2	1.160 ± 0.028	CCSVT	thermal	100	90 min	humid O_2	0.7
				200	70 min	O_2	0.7
#1a	1.032 ± 0.025	CCSVT	native	25	6 months	ambient air	1013
#2a	1.160 ± 0.028	CCSVT	native	25	6 months	ambient air	1013
#3	1.079 ± 0.026	CVD	native	25	4 months	ambient air	1013
#3a	1.079 ± 0.026	CVD	native	25	10 months	ambient air	1013
#4	1.033 ± 0.025	CVD	native	25	16 months	ambient air	1013

Table 2: Surface composition of as prepared $CuGaSe_2$ films, obtained by XPS line intensity analysis and bulk composition, determined by XRF and HI-ERDA, compared to literature data [15]. All data are given relative to the Cu content, which is set to one. Relative error for XRF and XPS values is 5% and ~10%, respectively.

sample	growth method	Cu (XRF)	Ga (XRF)	Se (XRF)	Na (HI-ERDA)	Cu2p (XPS)	Ga2p (XPS)	Se3d (XPS)	Na1s (XPS)
#1	CCSVT	1	1.03	1.98	0.04[a]	1	2.64	5.84	1.75
#2	CCSVT	1	1.16	2.16	0.04[a]	1	4.34	6.53	1.36
[15]	CVD	1	1.02	2.03	0.0024[b]	1	2.22	4.00	0.2
[15]	CVD	1	1.08	2.10	0.0024[b]	1	2.86	5.43	0.6

[a] The Na bulk concentration of 1at% [9] was related to the Cu content set to 1

[b] The Na bulk concentration of 0.06at% [15] was related to the Cu content set to 1

(XRF) thus showing a Cu depletion. The existence of a Cu-depleted near surface region for stoichiometric and Ga-rich grown $GuGaSe_2$ films (see table 2, [9] and [15]) as well as stoichiometric and In-rich $CuInSe_2$ films [17] is well known from literature. The bulk Na content of CCSVT thin films is far below the detection limit of XRF. It was determined by Heavy ion elastic recoil detection analysis (HI-ERDA) to an amount of 1at% [9], which corresponds to a value of 0.04 compared to Cu (see table 2). Thus, the surfaces of sample #1 and #2 are Cu-depleted and enriched in Ga, Se and Na.

3.1 Native oxidation

In the following the effect of native oxidation in air under ambient conditions is shown. The $Cu2p_{3/2}$ spectra of thin films after different times of native oxidation are plotted in figure 1. The as prepared film only reveals the typical $Cu2p_{3/2}$ peak of $CuGaSe_2$ with $E_B = 932.2$eV [15]. After native oxidation for 4 months a shift to $E_B = 932.6$eV is observed (Fig. 1b). A shift of the $Cu2p_{3/2}$ peak to higher binding energies was also found after thermal oxidation of

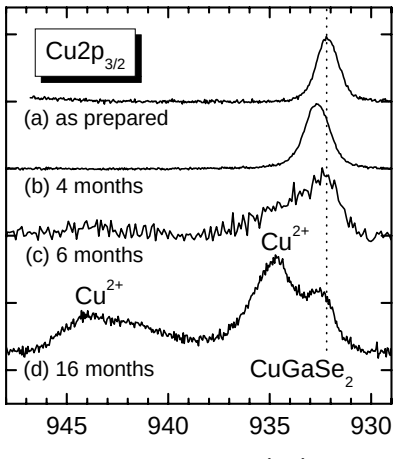

Figure 1: $Cu2p_{3/2}$ spectra of $CuGaSe_2$ thin films after native oxidation, (a) #2 as prepared, (b) #3 after 4 months, (c) #2a after 6 months and (d) #4 after 16 months oxidation. All spectra were measured in vacuum at 25°C, in (a) and (b) with synchrotron radiation ($h\nu = 1234$eV), in (c) and (d) with MgK_α radiation ($h\nu = 1253.6$ eV). The spectra were normalized to get similar intensities for the $Cu2p_{3/2}$ peak.

Table 3: XPS binding energy for the $Cu2p_{3/2}$ peak, its satellite band, difference of both, kinetic energy of the Cu LVV Auger peak and Auger parameter given in eV (with uncertainty ±0.2eV) measured at oxidized $CuGaSe_2$ samples compared to literature data for $Cu(OH)_2$, CuO, Cu_2O, Cu^0, $CuGaSe_2$ and $CuCO_3$

sample	$Cu2p_{3/2}$	satellite band		difference		Cu(LVV)	α
#2a	934.1					917.3	
#4	934.8	940.9	943.9	6.1	9.1	915.9[a]	1850.7
$Cu(OH)_2$	934.4[b]	940.6[b]	943.4[b]	6.2[b]	9.0[b]	916.3[c]	1850.7
CuO	933.8[b]	941.6[b]	944.0[b]	7.8[b]	10.2[b]	918.2[c]	1852.0
	933.5[d]					917.9[d]	1851.4
Cu_2O	932.5[b]					916.7[c]	1849.2
	932.2[d]					917.4[d]	1849.6
Cu^0	932.5[b]					919.0[c]	1851.5
	932.4[d]					918.6[d]	1851.0
$CuGaSe_2$	932.2[e]					917.0[f]	1849.2
$CuCO_3$	935.0[d]					916.3[d]	1851.3

$CuInSe_2$ and was attributed to the formation of a $Cu_{2-x}Se$ phase [5]. With further oxidation time a second structure appears at $E_B = 934.8$ eV connected with a satellite band that consists of two lines at $E_B \approx 941$ eV and 944 eV (Fig. 1c and d). These satellite peaks are a characteristic feature for paramagnetic Cu^{2+} [18]. Since XPS is extremely sensitive to small changes in the local binding configuration, it is possible to distinguish between the various Cu oxidation products that might exist after oxidation. For instance, the $Cu2p_{3/2}$ peak of $Cu(OH)_2$ is shifted in comparison to CuO by about 0.6 eV to higher binding energy [19], which can be reliably detected in the XP-spectra. From the analysis of the spectra as plotted in table 3, we find that the experimentally determined values for the binding energy of the $Cu2p_{3/2}$ line are in better agreement with what has been reported for $Cu(OH)_2$ rather than to CuO, in particular with regard to the distance of the satellite peaks to the $Cu2p_{3/2}$ peak. From this observation we propose, that native oxidation of copper at the surface of $CuGaSe_2$ films results in a $Cu(OH)_2$ phase.

The corresponding Ga3d spectra after different times of native oxidation are shown in Fig. 2. The as prepared sample exhibits only the typical Ga3d peak of $CuGaSe_2$ with a binding energy $E_B = 19.4$ eV [15]. A shift of the line to $E_B = 20.1$ eV is observed after native oxidation. This is indicative of Ga_2O_3 in the near-surface region ($E_B = 20.4$ eV) [22]. The Ga $L_3M_{45}M_{45}$ Auger spectra (not shown here) also support the formation of Ga_2O_3. The spectra of the oxidized samples show a peak with a kinetic energy $E_{kin} = 1062.4$eV characteristic for Ga_2O_3 [23] beside the $CuGaSe_2$ related peak at $E_{kin} = 1065.6$eV [24].

The native oxidation process also involves Se as can be seen from the Se3d spectra of the films (solid curves in Fig 3). The spectrum of the as prepared sample consists of the well known Se3d doublet structure (Fig. 3a) due to the spin-orbit splitting of the 3d electrons into a $3d_{5/2}$ ($E_B = 53.7$ eV) and a $3d_{3/2}$ level ($E_B = 54.6$ eV). After an

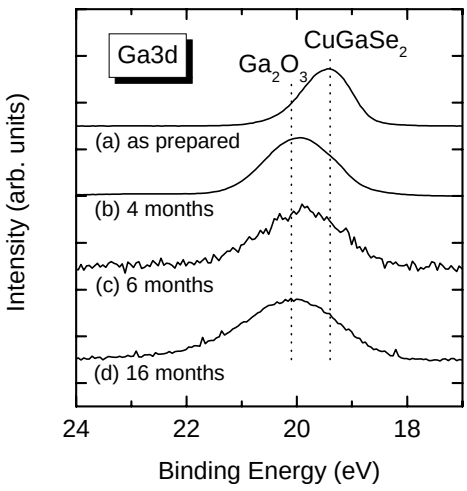

Figure 2: Ga3d spectra of $CuGaSe_2$ thin films after native oxidation, (a) #2 as prepared, (b) #3 after 4 months, (c) #2a after 6 months and (d) #4 after 16 months oxidation. All spectra were measured in vacuum at 25°C, in (a) and (b) with synchrotron radiation ($h\nu = 318$eV), in (c) and (d) with MgK_α radiation ($h\nu = 1253.6$ eV). The spectra were normalized to get similar intensities for the Ga3d peak.

oxidation time of 4 months a peak at $E_B = 58.8$ eV arises that increases with increasing oxidation time and can be assigned to SeO_2 [25]. Simultaneously, the Se3d peak has broadened and can be fitted by two sets of doublets, namely the doublet related to the $CuGaSe_2$ phase as well as by a second doublet shifted by 0.9eV to higher binding energies. This second doublet structure at $E_B = 54.9$eV is attributed to the formation of elemental Selenium Se^0 ($E_B = 55.1$eV, [26]) and/or a $Cu_{2-x}Se$ phase. For $CuInSe_2$ it is well known, that a $Cu_{2-x}Se$ phase forms at the interface between a binary In_2O_3 oxide phase and the ternary chalcopyrite bulk phase [5]. Kazmerski et al. [5] found, that the Cu2p and Se3d

Table 4: XPS binding energy values for the Na1s, Na2s, C1s and O1s peak and kinetic energy values for the Na KLL Auger peak and the corresponding Auger parameter α for the Na compound on oxidized $CuGaSe_2$ thin film surfaces compared to some possible sodium compounds

Sample or compound	Na1s	Na(KLL)		C1s	O1s	Na2s
	E_B/eV	E_{kin}/eV	α/eV	E_B/eV	E_B/eV	E_B/eV
#1, as prepared	1072.0				531.4	63.3
#1, thermal oxidation at 200°C	1071.9			289.2	531.5	63.5
#1, thermal oxidation at 300°C	1072.2				531.7	63.8
#3, native oxidation (4 months)	1072.0			289.2	531.4	63.6
#1a, native oxidation (6 months)	1071.5	989.9	2061.4	288.4	531.5	63.0
#2a, native oxidation (6 months)	1071.5	989.9	2061.4	288.5	531.4	63.0
Na_2CO_3 [a]	1071.5	989.8	2061.3	289.4	531.6	
$NaHCO_3$ [a]	1071.3	989.8	2061.1	290.0		
Na_2O [a]	1072.5	989.8	2062.3		529.7	64.2
Na_2SeO_3 [a]	1070.8	991.0	2061.8			
Na on $Cu(In,Ga)Se_2$ [b]	1072.3				531.7	

[a] values from reference [30]

[b] values for oxygen passivated Na on air exposed $Cu(In,Ga)Se_2$ from reference [31]

Table 5: Surface composition in at% of as prepared and oxidized $CuGaSe_2$ thin films estimated from XPS line intensity analysis compared to nominal composition of different oxide compounds; for carbon only the XPS peak at 288.5eV related to Na_2CO_3 was included; the values for the measurements with MgK_α radiation reveal a big error bar due to different information depths for the different peaks.

sample	Oxide	X-ray-source	t_{ox} / months	Cu2p	Ga2p	Se3d	Na1s	O1s	C1s
#1	as prepared	BESSY	-	7.2	18.9	41.9	12.5	19.5	0.0
#2	as prepared	BESSY	-	5.9	25.7	38.7	8.1	21.6	0.0
#1	thermal 200°C[a]	BESSY	-	0.3	8.8	3.7	32.9	54.0	0.2
#2	thermal 200°C[a]	BESSY	-	0.4	5.5	3.8	26.5	59.8	4.0
#1	thermal 300°C[b]	BESSY	-	0.1	14.9	2.3	17.9	64.7	0.0
#1a[c] (CCSVT)	native	MgK_α	6	1.0	0.5	1.5	27.2	53.0	16.9
#2a (CCSVT)	native	MgK_α	6	1.9	3.2	4.5	13.0	59.0	18.5
#3 (CVD)	native	BESSY	4	4.9	17.6	19.7	2.1	53.8	1.9
#3a (CVD)	native	MgK_α	10	4.1	10.6	6.9	4.0	67.3	7.2
#4 (CVD)	native	MgK_α	16	5.7	3.8	7.2	5.9	67.1	10.3
Ga_2O_3					40.0			60.0	
Na_2O/Ga_2O_3					25.0		25.0	50.0	
Na_2SeO_3						16.7	33.3	50.0	
Na_2CO_3							33.3	50.0	16.7

[a] The spectra were measured in gaseous O_2 atmosphere during thermal oxidation at 200°C.

[b] The spectra were measured at 300°C in vacuum after the thermal oxidation was finished.

[c] In the spectra of sample #1a neither Ga_2O_3, SeO_2 nor $Cu(OH)_2$ was detected

binding energy for the $Cu_{2-x}Se$ phase were shifted by 0.6 eV and 0.7 eV to higher values compared to $CuInSe_2$, respectively. Similar shifts for copper selenide compared to $CuInSe_2$ were also found by other groups [27, 28].

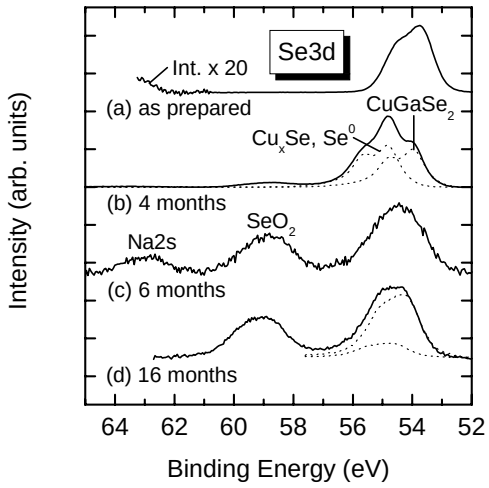

Figure 3: Se3d spectra of $CuGaSe_2$ thin films after native oxidation, (a) #2 as prepared, (b) #3 after 4 months, (c) #2a after 6 months and (d) #4 after 16 months oxidation. All spectra were measured in vacuum at 25°C, in (a) and (b) with synchrotron radiation ($h\nu = 354$eV), in (c) and (d) with MgK_α radiation ($h\nu = 1253.6$ eV). The dotted lines show fit curves. The spectra were normalized to get similar intensities for the Se3d peak.

The Se3d spectrum of sample #2a (Fig. 3c) measured clearly shows the Na2s peak at $E_B = 63.0$eV. In the spectrum of the corresponding as prepared sample #2 (Fig. 3a) this Na2s peak can only be seen when enlarging the spectrum by a factor of 20. As both spectra are measured with different photon energies and normalized to equal intensities for the Se3d peak, the intensities of both spectra cannot be compared directly. Nevertheless we observe an increase of the Na2s peak after oxidation also by taking into consideration the different information depths and the different photoionization cross sections. This increase of the sodium content at the surface after native oxidation is a hint, that sodium is also involved in the oxidation process. To find out, which sodium compound forms during oxidation, the XPS energy values for different Na containing compounds are listed in table 4 besides the measured values for our oxidized $CuGaSe_2$ samples. The comparison of these binding energies suggests the formation of sodium carbonate, Na_2CO_3, during native oxidation of $CuGaSe_2$ surfaces. Na_2CO_3 was also found after native oxidation of $Cu(In,Ga)Se_2$ thin films [29]. An estimation of the surface composition of the oxidized samples obtained by XPS line intensity analysis is shown in table 5. The increase in the sodium content at the surface is more pronounced for the CCSVT samples, which also show a higher sodium content at the as prepared surface (see table 2 and Fig. 3, the spectrum of the CCSVT sample #2a in Fig. 3c clearly shows the Na2s peak in contrast to that of the CVD sample #4 in Fig. 3d). The sample with the highest sodium surface content after native oxidation (#1a) neither showed formation of Ga_2O_3, SeO_2 nor $Cu(OH)_2$ (not shown). The surface composition of this sample is close to the nominal value one expects for Na_2CO_3 (see table 5). From this we conclude, that a protective oxide layer of Na_2CO_3 formed on the surface of sample #1a, which prevents further oxidation of the other elements.

We conclude, that during a 4 months native oxidation process binary oxides, predominantly Ga_2O_3 and some amount of SeO_2 were formed. Further we observed formation of $Cu_{2-x}Se$ and/or Se^0, but not of any copper oxide phase. Only after oxidation for longer than 4 months we were able to detect $Cu(OH)_2$ in the near-surface region. Additionally Na_2CO_3 was detected. The higher the sodium content of the as prepared surface, the higher is the amount of Na_2CO_3 and the lower is the amount of the other oxides.

3.2 Thermal oxidation

We will now focus on the thermal oxidation process studied in-situ with synchrotron radiation. After XPS measurement of its untreated as prepared surface the stoichiometric sample (#1) was oxidized in-situ under humid oxidizing conditions ($p(O_2) = 0.5$mbar and $p(H_2O) = 0.2$mbar) at 100°C, and in dry oxygen atmosphere at 200°C and 300°C (see table 1). The surface concentration of the different elements was determined from the spectra measured in vacuum at T_{ox} after the oxidation was finished. These surface concentrations normalized to the Cu content of the as prepared surface (set to one) are shown in Fig. 4. The Cu content (squares in Fig. 4) strongly decreases with oxidation temperature T_{ox}. After oxidation no shift in binding energy was observed for the $Cu2p_{3/2}$ and $Cu(L_3VV)$ Auger peak (not shown) compared to the as prepared surface. The Se content at the surface (open triangles in Fig. 4) also decreased with T_{ox}. Only traces of SeO_2 were found in the spectra measured in vacuum (see Fig. 7 and Fig. 8 below). The Ga content at the surface (open circles in Fig. 4) increased with T_{ox} parallel to the oxygen content (filled triangles in Fig. 4). The higher the oxidation temperature T_{ox}, the more the Ga3d peak shifts to higher binding energies reaching $E_B = 20.3$eV after oxidation at 300°C. This binding energy corresponds to the value reported for Ga_2O_3 ($E_B = 20.4$eV) [22] indicating the oxidation of Ga. The Ga $L_3M_{45}M_{45}$ Auger spectra (not shown here) support the formation of Ga_2O_3. A feature at $E_{kin} = 1062.5$eV characteristic for Ga_2O_3 [23] grows up with T_{ox}. The Na content at the surface (rhombs in Fig. 4) also increases with T_{ox} and then slightly decreases at $T_{ox} = 300$°C. The binding energy of $E_B = 1072.0$eV for the Na1s level remained unchanged with T_{ox}. The increase in intensity parallel to that of oxygen suggests the formation of a sodium oxide compound at the surface. Comparing the measured binding energies with that of different sodium

oxide compounds (table 4) suggests the formation of Na_2CO_3 like in case of the native oxides. But Na_2CO_3 cannot be the main sodium oxide compound, as the surface concentration of carbon (stars in Fig. 4) does not increase with T_{ox} like sodium. The estimated surface composition of the stoichiometric sample (#1) after oxidation at $T_{ox} = 300°C$ is 0.1% Cu, 14.9% Ga, 2.3% Se, 17.9% Na, 64.7% O and 0.0% C (see table 5). These values better fit to a mixture of Na_2O and Ga_2O_3 with a nominal surface composition of 25% Na, 25% Ga and 50% O. Therefore for the thermal oxide we propose the formation of Na_xO and only small amounts of Na_2CO_3.

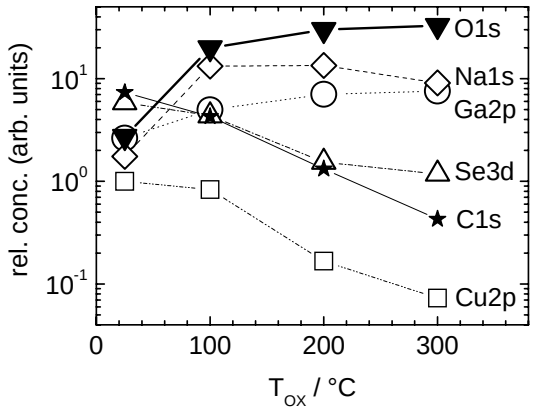

Figure 4: Surface composition of the stoichiometric sample (#1) as prepared ($T_{ox} = 25°C$) and after thermal oxidation at different temperatures T_{ox}. The relative surface concentration of the different elements was determined from $Cu2p_{3/2}$ (square), Ga2p (circle), Se3d (open triangle), Na1s (rhomb), O1s (filled triangle) and C1s (star) peak areas of sample #1 measured in vacuum at T_{ox} after the oxidation was finished. The values are normalized to the Cu content of the as prepared surface ($T_{ox} = 25°C$), which is set to one.

The XPS spectra of the Ga-rich sample (#2) after thermal oxidation (not shown) reveal the same changes at the surface as found for the stoichiometric sample #1. The surface composition after thermal oxidation at 200°C resembles that of sample #1 (see table 5). The Cu and Se content at the surface exponentially decreases with T_{ox}, whereas the Na, Ga and O content increases (Fig. 4). This suggests the formation of an oxide layer consisting of Na_xO and Ga_2O_3 covering the $CuGaSe_2$ film surface. In this case the O1s signal should contain contributions from Ga_2O_3 and Na_xO. The O1s spectra of sample #1 after different oxidation steps are shown in figure 5a. The peak maximum shifts from $E_B = 531.4eV$ to 531.7eV when increasing the oxidation temperature T_{ox}. The O1s spectra can be fitted by three peaks with gauss profile (Fig. 5b) located at $E_B = 532.9eV$, 531.8eV and 530.7eV. The change of peak area of these three components in dependence of T_{ox} is illustrated in Fig. 6. The component with the lowest intensity located at $E_B = 532.9eV$ (triangle in Fig. 6) is attributed to chemisorbed hydroxide, OH^- [32], as it strongly in

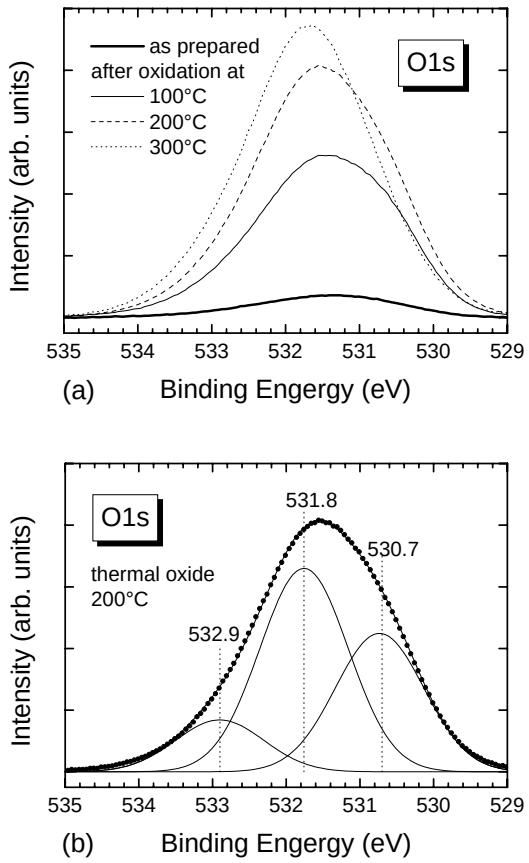

Figure 5: (a) O1s spectra of the stoichiometric sample (#1) as prepared ($T_{ox} = 25°C$, bold solid curve) and after thermal oxidation at 100°C (solid curve), 200°C (dashed curve) and 300°C (dotted curve) measured with synchrotron radiation ($h\nu = 830eV$) in vacuum at T_{ox} after oxidation was finished. (b) Fit of the O1s spectrum measured at $T_{ox} = 200°C$ (dashed curve in (a)) with three gauss profiles.

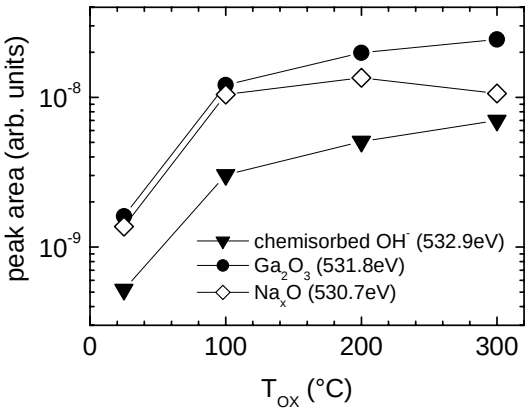

Figure 6: Peak area of the three oxygen components (shown in Fig. 5b) obtained by fitting the O1s spectra of the stoichiometric sample (#1) measured in vacuum at T_{ox} after thermal oxidation was finished; component located at $E_B = 532.9eV$ (triangle), $E_B = 531.8eV$ (circle) and $E_B = 530.7eV$ (rhomb).

creases after the oxidation step under humid oxygen atmosphere at T_{ox} = 100°C. The peak located at E_B = 531.8eV (circle in Fig. 6) is connected to Ga_2O_3 as its binding energy is close to the literature value of E_B = 531.5eV for Ga_2O_3 [33] and as it increases monotonously with T_{ox} like the Ga2p peak (see Fig. 4). The area of the peak located at E_B = 530.7eV (rhomb in Fig. 6) first increases with T_{ox} and then decreases at T_{ox} = 300°C. The same behavior was observed for the Na1s peak (rhomb Fig. 4). Therefore we attribute this third peak to Na_xO. The binding energy of E_B = 1072.0eV for the Na1s peak of the as prepared and thermally oxidized samples (see table 4) corresponds to the value reported for an oxygen passivated Na specie at the surface of air exposed $Cu(In,Ga)Se_2$ thin films (see table 4 and [31]). The formation of Na_2O cannot directly be concluded from our experiments as we did not measure the Na(KLL) spectrum to determine the Auger parameter and as the energy values for Na1s, Na2s and O1s peak all deviate from the reported values for Na_2O (see table 4). The O1s spectra of the as prepared thin film (T_{ox} = 25°C in Fig. 6) also contains the three different oxygen components, revealing that formation of Ga_2O_3 and Na_xO already takes place after exposure of the thin film surface to ambient air for some minutes (during mounting on the sample holder). From the peak area of the different components we get quantitative information about the oxide phases. Assuming that all Na atoms of the as prepared surface of sample #1 are oxidized, we estimate a composition of $Na_{1.7}O$ for the sodium oxide compound, which is closes to the nominal value for Na_2O. From the oxygen peak related to Ga_2O_3 we estimate that 7% of the Ga atoms of the as prepared surface are oxidized.

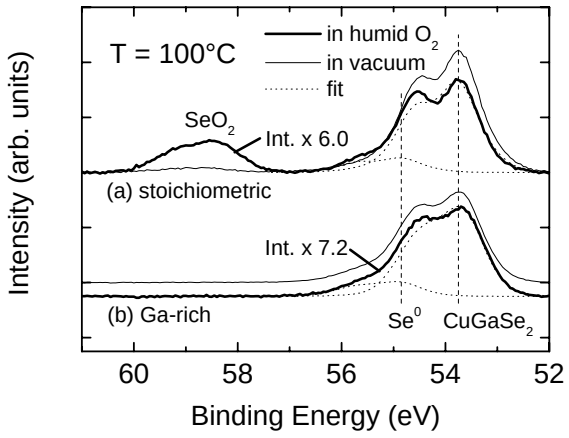

Figure 7: Se3d spectra measured at T_{ox} = 100°C with synchrotron radiation (hν = 354eV) in humid oxygen (bold solid curves) and in vacuum (solid curves) after exposure to humid oxygen of (a) Ga-rich sample #2 and (b) stoichiometric sample #1. The dotted lines are fits for the curves in humid oxygen. The solid curve in (b) is shifted up to better compare it to the bold solid curve.

From the exponential decrease of the $Cu2p_{3/2}$ peak area (Fig. 4) it is possible to estimate the thickness of the complete oxide layer. With an inelastic mean free path of 8Å for photoelectrons with E_{kin} = 300eV [34] we estimate a thickness of 2nm for the oxide layer after the oxidation at 300°C.

As the XPS chamber allowed to measure spectra under gaseous conditions, they will now be compared with those measured under vacuum conditions. For this purpose the spectra measured under gaseous conditions, which show lower signal intensity, are normalized. As the line shape of the Ga3d spectra essentially remained unchanged all spectra measured under gaseous conditions were multiplied with a factor obtained by normalizing the Ga3d spectra. After this normalizing procedure the $Cu2p_{3/2}$ spectra essentially remained unchanged (not shown). The main changes were observed in the Se3d spectra. At 100°C the Se3d spectrum of the stoichiometric sample (#1) measured in humid oxygen differs from that measured in vacuum (Fig. 7a). The spectrum detected in humid oxygen (bold solid curve in Fig. 7a) clearly shows a SeO_2 peak at E_B = 58.9eV. A fit of the Se3d feature measured in humid O_2 (bold curve in Fig. 7a) with the Se3d doublet spectrum of the untreated sample (dotted curves in Fig. 7a) reveals that beside the $CuGaSe_2$ related doublet at $E_B(Se3d_{5/2})$ = 53.7eV the spectrum contains another doublet shifted by 1.1eV to higher binding energies. This can be attributed to elemental Selenium, Se^0, which is reported to have $E_B(Se3d_{5/2})$ = 55.1eV [26]. In the spectrum measured in vacuum (solid curve in Fig. 7b) only a small amount of the SeO_2 peak and the Se^0 related doublet remains whereas the $CuGaSe_2$ related doublet increased. Hence, the heat treatment of the stoichiometric sample (#1) in vacuum at 100°C strongly changes the Se3d spectra. This is in strong contrast to the Se3d spectra of the Ga-rich sample (#2) measured under similar conditions (Fig. 7b). A fit of the spectra in Fig. 7b with the line shape of the untreated sample reveals that it also contains the Se^0 related doublet with $E_B(Se3d_{5/2})$ = 54.9eV beside the $CuGaSe_2$ related doublet. But the formation of SeO_2 was not observed on the surface of the Ga-rich sample (#2) at 100°C.

Thermal oxidation at 200°C leads to the formation of SeO_2 on the surface of the Ga-rich sample (Fig. 8a) with the same amount as for the stoichiometric sample (Fig. 8b). Its intensity increases compared to the 100°C spectra and in relation to the main peak. The spectra at 200°C also contain the Se^0 related doublet at $E_B(Se3d_{5/2})$ = 54.7eV. Under vacuum conditions at 200°C both the SeO_2 peak and the shifted Se^0 related doublet strongly diminish while the $CuGaSe_2$ related doublet increases (Fig. 8b). After thermal oxidation of the stoichiometric sample (#1) at 300°C no SeO_2 peak appears neither in the spectrum measured in O_2 atmosphere nor in vacuum (Fig. 8c). The spectrum measured in O_2 atmosphere almost overlaps with that acquired in vacuum. The doublet structure of the Se3d peak becomes broader. The spectrum measured in O_2 atmosphere (bold solid curve in Fig. 8c) can be fitted with the $CuGaSe_2$ related doublet and another doublet shifted by 0.4eV to higher binding energies. This shifted doublet at $E_B(Se3d_{5/2})$ = 54.1eV can be attributed to $Cu_{2-x}Se$ [5].

Table 6: Standard molar enthalpy (heat) of formation $\Delta_f H^0$ at 298.15K in kJ/mol of different compounds [38-40]

comp.	Na_2CO_3	Ga_2O_3	Na_2SeO_3	$Cu(OH)_2$	Na_2O	SeO_2	Cu_2O	CuO	Cu_2Se	CuSe
$\Delta_f H^0$	1130.7	1089.1	990.6[a]	449.8	414.2	225.4	168.6	157.3	65.26[b]	39.5

[a] From reference [39]
[b] From reference [40]

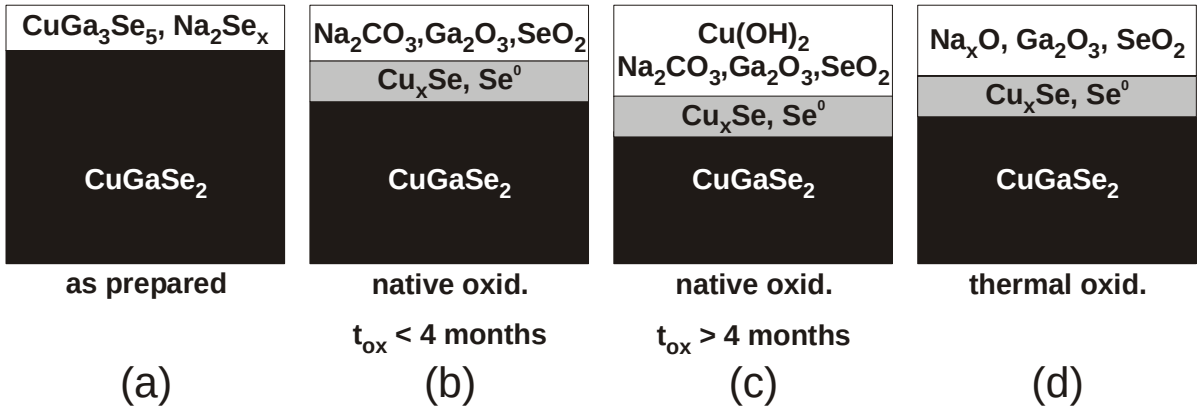

Figure 9: Model for the oxidation of $CuGaSe_2$ (a) as prepared and not exposed to air, (b) after short term native oxidation (t_{ox} < 4 months), (c) after long term native oxidation (t_{ox} > 4 months) and (d) after thermal oxidation.

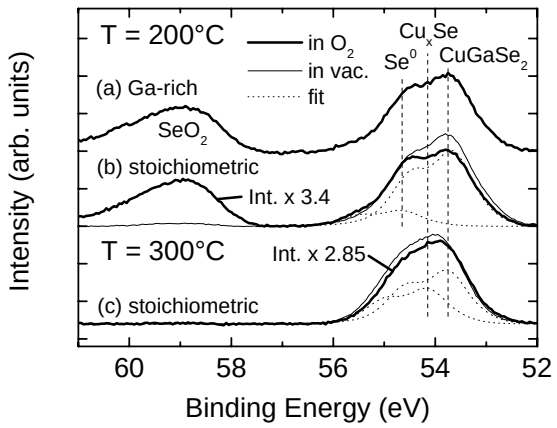

Figure 8: Se3d spectra measured with synchrotron radiation (hν = 354eV) in O_2 (bold solid curves) and in vacuum (solid curves) after oxidation was finished of (a) Ga-rich sample #2 at 200°C and (b) stoichiometric sample #1 at 200°C and (c) sample #1 at 300°C. The dotted lines are fits for the curves in O_2-atmosphere.

We conclude, that thermal oxidation of $CuGaSe_2$ results in the formation of an oxide layer consisting of sodium oxide and Ga_2O_3 at the $CuGaSe_2$ thin film surface. Additionally traces of Na_2CO_3 are observed. In the spectra measured under gaseous conditions SeO_2 and Se^0 are found, which both strongly decrease during thermal treatment in vacuum. After oxidation at 300°C a component attributed to Cu_xSe was revealed. Formation of copper oxides was not detected.

4. Discussion

Generally, the driving force for the growth of oxide layers on metal and semiconductor solid state surfaces is the minimization of the surface free-energy of the system, since the surface free energies of oxides are much lower than for the metals or semiconductors. Thus, metals and semiconductors are always covered by a substance which lowers the free surface energy of the system. Usually, they are covered by ultra thin layers of hydrocarbons, oxides often also by water (OH groups) [35].

According to the photoemission results we propose a simple model for the native oxidation of $CuGaSe_2$ as shown in figure 9. The surface of the as prepared thin films shows a copper-depleted surface composition of about $CuGa_3Se_5$ (Fig. 9a and table 2). Additionally sodium polyselenide Na_2Se_x (x > 2) is assumed to be at the surface, which is supposed to serve as Se-reservoir during growth of $CuGaSe_2$ [36, 37]. This Na_2Se_x forms during growth of $CuGaSe_2$ by reaction of H_2Se from the reacting gas phase with Na^+ diffusing out from the soda lime glass substrate through the Mo layer. The native oxidation already starts during short exposure of this surface to air for some minutes during mounting on the sample holder. The Na_2Se_x is immediately oxidized to Na_2O and small amounts of Ga_2O_3 are formed. When further exposing the surface to air the oxidation process proceeds with the growth of the thermodynamically most stable Na_2CO_3 and Ga_2O_3 (see table 6 and [38]). The amount of Na_2CO_3 in relation to Ga_2O_3 is the higher, the higher the Na content on the as prepared

surface is. As the CCSVT samples exhibit a higher Na content at the as prepared surface (table 2), the Na_2CO_3 content after oxidation is also higher compared to the CVD samples (table 5). In case of very high sodium content on the surface Na_2CO_3 can even prevent oxidation of the other elements (see #1a in table 5). This is in accordance with the results of Braunger et al. [37] who found a lower amount of Ga_2O_3 and In_2O_3 on $Cu(In,Ga)Se_2$ layers grown on soda lime glass compared to layers grown on Na free substrates. After formation of Na_2CO_3 and Ga_2O_3 the remaining Cu and Se readjust at the interface to form elemental Se^0 and an interfacial $Cu_{2-x}Se$ layer (Fig. 9b). Additionally, SeO_2 is formed. During a "long term" oxidation process of more than 4 months the amount of this SeO_2 phase increases (Fig. 9c) and $Cu^{2+}(OH^-)_2$ is formed as fourth oxide phase. The small Cu^+ ions of the bulk diffuse from the bulk Cu_x-Se/oxide or $CuGaSe_2$/oxide interface towards the surface of the already existing native oxide layer consisting of Na_2CO_3, Ga_2O_3 and SeO_2. This copper transport through the oxide layer is mediated via cationic vacancies either inside the bulk of the native oxide layer or in the grain boundaries [41]. At the surface of the native oxide these Cu^+ ions react with the hydroxyl groups of the adsorbed water to form an outwardly growing $Cu^{2+}(OH^-)_2$ layer. According to the higher standard molar enthalpy (heat) of formation of $Cu(OH)_2$ compared to SeO_2 (see table 6) one would expect that the growth of $Cu(OH)_2$ already occurs during short term oxidation process before SeO_2 is formed, which was not observed here for the thin films. The Cu depletion of as grown film surfaces accompanied by a Se rich surface composition favors the growth of SeO_2 instead of the formation of $Cu(OH)_2$.

The detailed analysis of the growth mechanism of thermal oxide layers on $CuGaSe_2$ surfaces was enabled by the possibility to measure PE-spectra in-situ, i. e. under gaseous conditions. The oxide growth starts with the formation of a sodium oxide compound Na_xO and Ga_2O_3, the two thermodynamically stable compounds already observed on the as prepared surface (see Fig. 5 and 6), followed by the formation of SeO_2. By the Se3d spectra measured in gaseous atmosphere (bold solid curves in Fig. 7 and 8) it was possible to observe the different oxidation states of Se. We conclude, that Se^{2-} of the chalcopyrite (E_B ($Se3d_{5/2}$)= 53.7eV) is stepwise oxidized via metallic Se^0 (E_B ($Se3d_{5/2}$) = 54.8eV) to Se^{4+} of SeO_2 (E_B = 58.8eV). Thermal treatment in vacuum (solid curves in Fig. 7 and 8) removes the oxide and only traces of SeO_2 and Se^0 could be detected. This can be explained by sublimation of SeO_2 and Se^0 solid state phase at $T \geq 100°C$ due to the high vapor pressures of SeO_2 and Se^0 [42]. At 300°C the high vapor pressure of 335mbar for SeO_2 [40] even exceeds that of the gas atmosphere with $p(O_2) = 0.7$mbar. Therefore, the SeO_2 related feature was not found in the spectra measured at 300°C neither in gas atmosphere nor in vacuum (Fig. 7c). Finally the $Cu_{2-x}Se$ related doublet remained in the Se3d spectra measured at 300°C (Fig. 7c).

The formation of SeO_2 and Se^0 was found to depend on the surface composition and the temperature. On a Ga-rich surface (sample #2) thermal oxidation at 100°C is not favoring the growth of SeO_2. At 200°C the thermal oxide of the Ga-rich surface has the same composition like that of the stoichiometric sample (#1, see table 5). This is a hint, that a high amount of Ga at the surface favors the oxidation of Ga before Se is oxidized, in accordance with the enthalpy of formation (see table 6).

The main difference of the thermal in contrast to the native oxidation process is the different oxidation behavior of sodium and copper. Neither $Cu(OH)_2$ nor copper oxides have been found after thermal oxidation. That no CuO or Cu_2O formed can be explained by the fact, that these oxides are less stable than Ga_2O_3 and SeO_2 (see table 5). The Cu depletion of thin film surfaces further inhibits growth of copper oxides. Further the formation of $Cu(OH)_2$ at elevated temperatures is improbable, as $Cu(OH)_2$ is dehydrogenated at $T > 100°C$ [43] and can be easily reduced to Cu_2O by annealing at $T > 100°C$ [44, 45]. The other difference between thermal and native oxides is, that sodium reacts to Na_2CO_3 during native oxidation, whereas on thermal oxides mainly Na_xO and only small amounts of Na_2CO_3 were detected. This can be explained by fact that during thermal oxidation CO_2 from ambient air is missing, so that only Na_xO can be formed. Even the high amount of adsorbed hydrocarbons found on the as prepared samples (see Fig. 4) cannot induce formation of Na_2CO_3 during thermal oxidation. The hydrocarbons are oxidized to CO_2, which desorbs from the surface at higher temperatures, explaining the decrease of the C1s signal during thermal oxidation (stars in Fig. 4).

5. Conclusion

The novel design of our XPS setup enables us to monitor in-situ the growth of thin oxides on $CuGaSe_2$ thin films. The surface of as prepared $CuGaSe_2$ thin films is found to be copper depleted and enriched in Ga, Se and Na compared to the bulk composition. This favors the growth of sodium oxide compounds, Ga_2O_3 and SeO_2 when exposing the surface to oxidizing atmospheres during thermal as well as native oxidation. The main difference between the thermal and native oxidation process is the oxidation behavior of Cu and Na. Thermal oxides do no exhibit copper oxides, whereas native oxides show the formation of $Cu(OH)_2$ after oxidation in air under ambient conditions for longer than four months. During native oxidation Na at the film surface reacts to Na_2CO_3, whereas during thermal oxidation in oxygen atmosphere mainly Na_xO and only a small amount of Na_2CO_3 are formed. The higher the amount of the oxidic sodium compounds on the surface, the lower is the amount of other oxides. The different oxidation states of Se on the surface have been monitored by measuring XPS under oxidizing conditions. Exposure of the oxidized film surface to ultra high vacuum at $T \geq 100°C$ sublimates the oxidation products SeO_2 and Se^0.

Acknowledgements

We thank Rolf Follath for technical support at the BESSY II beamline U49/2 PGM1. Thanks to Jörg Reichardt and Alexander Grimm for performing XPS measurements with MgK_α radiation, to A. Meeder and D. Fuertes Marrón for preparation of thin films. This work was supported by the Bundesministerium für Wirtschaft Deutschland through its CCSVT-project (contract No. 0329740B), which is gratefully acknowledged.

References

[1] M. Saad, H. Riazi-Nejad, E. Bucher, M. C. Lux Steiner, in *1st World Conference on Photovoltaic Energy Conversion* (IEEE, Hawaii, 1994), p. 214.
[2] D. L. Young, J. Keane, A. Duda, J. A. M. AabuShama, C. L. Perkins, M. Romero, and R. Noufi, Prog. Photovolt: Res. Appl. **11**, (2003) 535.
[3] V. Nadenau, D. Hariskos, H. W. Schock, in *14th EC Photovoltaic Solar Energy Conference*, edited by H. Ossenbrink, P. Helm, H. Ehmann (Stephens & Associates, Barcelona, 1997), p. 1250.
[4] D. Hariskos, G. Bilger, D. Braunger, M. Ruckh, H. W. Schock, Inst. Phys. Conf. Ser No. 152: Section E: Surfaces and Interfaces (1997) 707, ICTMC-11.
[5] L. L. Kazmerski, O. Jamjoum, P. J. Ireland, S. K. Deb, J. Vac. Sci. Technol. 19 (1981) 467.
[6] L. L. Kazmerski, O. Jamjoum, J. F. Wagner, P. J. Ireland, K. J. Bachmann J. Vac. Sci. Technol. A 1 (1983) 668.
[7] A. J. Nelson, S. Gebhard, L. L. Kazmerski, E. Colavita, M. Engelhardt, H. Höchst, Appl. Phys. Lett. 57 (1990) 1428.
[8] I. Dirnstorfer, W. Burkhardt, W. Kriegseis, I. Österreicher, H. Alves, D. M. Hofmann, O. Ka, A. Polity, B. K. Meyer, and B. Braunger, Thin Solid Films 361-362 (2000) 400.
[9] M. Rusu, S. Wiesner, D. Fuertes Marrón, A. Meeder, S. Doka, W. Bohne, S. Lindner, Th. Schedel-Niedrig, Ch. Giesen, M. Heuken, M. Ch. Lux-Steiner, Thin Solid Films 451 (2004) 556.
[10] D. Fischer, N. Meyer, M. Kuczmik, M. Beck, A. Jäger-Waldau, and M. Ch. Lux-Steiner, Sol. Energy Mat. Sol. Cells **67**, 105 (2001).
[11] D. Fischer, T. Dylla, N. Meyer, M. E. Beck, A. Jäger-Waldau, and M. Ch. Lux-Steiner, Thin Solid Films **387**, 63 (2001).
[12] D. Fuertes Marrón, A. Meeder, R. Würz, S. M. Babu, Th. Schedel-Niedrig, and M. Ch. Lux-Steiner, PV in Europe, from PV technology to energy solutions, Conference Proceedings, Rome, Italy, 2002, p. 421, published by WIP Munich and ETA Florence.
[13] K. J. S. Sawhney, F. Senf, and W. Gudat, Nucl. Instrum. Methods A 467 (2001) 466.
[14] [14] H. Bluhm, M. Hävecker, A. Knop-Gericke, E. Kleimenov, R. Schlögl, D. Teschner, V. I. Bukhtiyarov, D. F. Ogletree, and M. Salmeron, J. Phys. Chem. B, 2004, in press; D. F. Ogletree, H. Bluhm, G. Lebedev, C. S. Fadley, Z. Hussain, and M. Salmeron, Rev. Sci. Instrum. 73 (2002) 3872.
[15] A. Meeder, L. Weinhardt, R. Stresing, D. Fuertes Marrón, R. Würz, S. M. Babu, T. Schedel-Niedrig, M. Ch. Lux-Steiner, C. Heske and E. Umbach, J. Phys. Chem. Sol. **64**, 1553 (2003).
[16] J. J. Yeh and I. Lindau, Atomic data an nuclear data tables 32 (1985) 1.
[17] D. Schmid, M. Ruckh, F. Grunwald, H. W. Schock, J. Appl. Phys. 73 (1993) 2902.
[18] L. Fiermans, R. Hoogewijs, and J. Vennik, Surf. Sci. 47 (1975) 1.
[19] N. S. McIntyre, M. G. Cook, Anal. Chem. 47 (1975) 2208.
[20] N. S. McIntyre, S. Sunder, D. W. Shoesmith, and F. W. Stanchell, J. Vac. Sci. Technol. 18 (1981) 714.
[21] C. D. Wagner, W. M. Riggs, L. E. Davis, and J. F. Moulder, in *Handbook of X-ray photoelectron spectroscopy*, edited by G. E. Muilenberg (Perkin Elmer, Eden Prairie, Minnesota 1978).
[22] G. Leonhardt, A. Berndtsson, J. Hedman, M. Klasson, R. Nilsson, C. Nordling, Phys. Stat. Sol. 60 (1973) 241.
[23] C. D. Wagner, Discuss. Faraday Soc. 60 (1975) 291.
[24] D. Schmid, M. Ruckh, and H. W. Schock, Appl. Surf. Sci. 103 (1996) 409.
[25] M. K. Bahl, R. L. Watson, and K. J. Irgolic, Anal. Chem. 51, (1979) 466.
[26] M. K. Bahl, R. L. Watson, and K. J. Irgolic, J. Chem. Phys. 72 (1980) 4069.
[27] D. Cahen, P. J. Ireland, L. L. Kazmerski, F. A. Thiel, J. Appl. Phys. 57 (1985) 4761.
[28] E. P. Domashevskaya, V. V. Gorbachev, V. A. Terekhov, V. M. Kashkarov, E. V. Panfilova, and A. V. Shchukarev, J. Electron Spectr. and Related Phenomena 114-116 (2001) 901.
[29] A. Kylner, Journal of Electrochemical Society 146 (1999) 1816.
[30] J. F. Moulder, W. F. Stickle, P. E. Sobol, and K. D. Bomben, *Handbook of X-Ray Photoelectron Spectroscopy*, (Perkin-Elmer Corp., Eden Prairie, Minnesota, 1992).
[31] C. Heske, G. Richter, Z. Chen, R. Fink, E. Umbach, W. Riedl, and F. Karg, J. Appl. Phys. 82 (1997) 2411.
[32] D. Y. Zemlyanov, E. Savinova, A. Scheybal, K. Doblhofer, and R. Schlögl, Surf. Sci. 418 (1998) 441.
[33] H. Iwakuro, C. Tatsuyama, S. Ichimura, Jpn. J. Appl. Phys. 21 (1982) 94.
[34] S. Tanuma, C. J. Powell, D. R. Penn, Surface and Interface Analysis 17 (1991) 911.
[35] A. Zangwill, *Physics at Surfaces* (Cambridge University Press, 1983); G. A. Somorjai, *Chemistry in Two Dimensions: Surfaces* (Cornell University Press, Ithaca, 1981).
[36] M. R. Balboul, U. Rau, G. Bilger, M. Schmidt. H. W. Schock, and J. H. Werner, J. Vac. Sci. Technol. A 20 (2002) 1247.
[37] D. Braunger, D. Hariskos, G. Bilger, U. Rau, H. W. Schock, Thin Solid Films 361 (2000) 161.
[38] J. D. Cox, D. D. Wagman and V. A. Medvedev, in *CRC Handbook of Chemistry and Physics 2001-2002: A Ready-Reference Book of Chemical and Physical Data*, edited by D.R. Lide (CRC Press, Boca Raton, Florida, USA, 82nd edition, 2001).
[39] R. J. Meyer and E. H. Erich Pietsch, *Gmelins Handbuch der anorganischen Chemie*, Natrium, Ergänzungsband 3, System Nr. 21, (Verlag Chemie, Weinheim/Bergstraße, 1966).
[40] O. Knacke, O. Kubaschewski, K. Hesselmann, in *Thermochemical properties of inorganic substances* (Springer, New York, 1991).
[41] H. Schmalzried, *Chemical Kinetics of Solids* (VCH Weinheim, 1995, ch. 6, p. 7).

[42] The vapor pressure of SeO_2 at 100°, 200° and 300°C is $8 \cdot 10^{-4}$, 2 and 335mbar, respectively [40]. The vapor pressure of Se at 100°C, 200°C and 300°C is $3 \cdot 10^{-8}$, $2 \cdot 10^{-3}$, and 0.3mbar, respectively [40].
[43] E. H. Erich Pietsch, *Gmelins Handbuch der anorganischen Chemie*, Kupfer Teil B, System Nr. 60, (Verlag Chemie, Weinheim/Bergstraße, 1958).
[44] R. Würz, A. Meeder, D. Fuertes Marrón, Th. Schedel-Niedrig, H. Bluhm, K. Lips, to be published.
[45] T. Robert, M. Bartel, G. Offergeld, Surf. Sci. 33 (1972) 123